POLITECNICO DI TORINO
Repository ISTITUZIONALE

Evaluation of Various Geometrical Nonlinearities in the Response of Beams and Shells

Terms of use:

(Article begins on next page)

28 March 2024

Evaluation of various geometrically nonlinear terms in the static response of beams and thin-walled shell-like structures

A. Pagani [*], E. Carrera [†] and R. Augello [‡]

MUL² group, Department of Mechanical and Aerospace Engineering,
Politecnico di Torino, Corso Duca degli Abruzzi 24, 10129 Torino, Italy.

This paper investigates the consistency and compatibility of various assumptions and strain measurements in large displacements/geometric nonlinear analysis of beams and thin-walled structures. For this purpose, a refined beam model with enhanced three-dimensional accuracy is employed, in a total Lagrangian scenario. This model is developed in the domain of the Carrera Unified Formulation (CUF), which allows to express the nonlinear governing equations in terms of fundamental nuclei. These nuclei are independent of the theory approximation order; thus, low- to high-order theories of structures can be implemented with ease. Various numerical problems are addressed, and solutions are provided by using a classical finite element method and a Newton-Raphson linearization scheme. Given the intrinsic scalable nature of CUF, investigating the effects of the various nonlinear strain components is straightforward. It is demonstrated that the full Green-Lagrange strain tensor produces good approximation in case of large rotations, post-buckling and nonlinear couplings. In contrast, approximations may be reasonable as moderate displacements and simpler problems (e.g., slender beams under flexure) are considered.

Nomenclature

$\mathbf{b}$	=	differential operator
F_τ, F_s	=	cross-sectional functions
$\mathbf{K}_S$	=	secant stiffness matrix
$\mathbf{K}_T$	=	tangent stiffness matrix
N_i, N_j	=	shape functions
$\mathbf{p}$	=	loading vector
$\mathbf{q}$	=	nodal unknowns
$\mathbf{u}$	=	displacement vector

---

[*]Assistant professor, Dept. of Mechanical & Aerospace Eng., Politecnico di Torino, AIAA Fellow. E-mail: alfonso.pagani@polito.it.
[†]Professor, Dept. of Mechanical & Aerospace Eng., Politecnico di Torino, AIAA Fellow.
[‡]PhD student, Dept. of Mechanical & Aerospace Eng., Politecnico di Torino.

δ	=	virtual variation
ϵ	=	strain vector
λ	=	load parameter
σ	=	stress vector

Subscripts

ext	=	external
int	=	internal
l	=	linear
nl	=	nonlinear
ref	=	reference

I. Introduction

Highly flexible structures are widely used in many engineering fields. These are structures that are designed to undergo large displacements/rotations without plastic deformations. Applications include, but are not limited to, inflatable structures, space antennas, parachutes, cables for cable-stayed bridges, helicopter rotor blades, and flexible wings of high altitude aircraft [1]. In this context, the availability of efficient and reliable numerical tools able to predict the nonlinear mechanical behaviour of this class of structures, which continues to propose challenging problems, is of fundamental importance for modern analysts.

First studies about highly flexible beams and cables date back to XVIII century, when Euler [2] proposed the well-known *elastica* to address flexural problems and by assuming local curvature as proportional to the bending moment. In his theory, geometrical nonlinearity was considered and analytical solutions that make use of elliptic integrals are available and used still today for clamped-free, clamped-clamped, and simply-supported beams (see [3, 4]). Starting from the original work of Euler, many theories for geometric nonlinear analysis of one-dimensional (1D) and two-dimensional (2D) structures have been developed. In fact, a review of the modern literature shows a vivid interest of engineers and researchers on this matter. For example, in a recent work, Sze *et al.* [5] provided solutions and benchmarks for different geometric nonlinear analyses of plates and shells by using finite elements (FE). Ovesy *et al.* [6] developed two versions of the finite strip method for the post-buckling response of rectangular symmetric and unsymmetrical laminates subjected to progressive end-shortening as well as normal pressure loading. Milazzo and Olivieri [7] discussed, on the other hand, a Ritz approach for the analysis of buckling and post-buckling of stiffened composite panels with through-the-thickness cracks and delaminations. Ma and Wang [8] investigated large deflections of functionally graded circular plates subjected to mechanical and thermal loadings by employing a classical nonlinear von Kármán plate theory. Other important and recent contributions addressing geometric nonlinear

problems of 2D structures are those by Arciniega *et al.* [9], who investigated buckling and post-buckling behaviour of laminated cylindrical shells under axial compression and lateral pressure; Arciniega and Reddy [10], who developed a tensor-based finite element formulation with curvilinear coordinates and first-order shear deformation theory to analyze large displacements of functionally graded shells; and Ko *et al.* [11], who demonstrated the effectiveness of a new shell element based on MITC (Mixed Interpolation of Tensorial Components) to eliminate locking phenomena in geometrical nonlinear analysis.

Many of the works on nonlinear theories of beam structures are based on the Timoshenko beam theory [12], which assumes a uniform shear distribution along the cross-section of the beam together with the effects of rotatory inertia, see for example Refs. [13–15]. In contrast, in the domain of the variational asymptotic method, the general three-dimensional nonlinear elasticity problem was systematically split into a two-dimensional linear cross-sectional analysis and a one-dimensional nonlinear beam analysis (including, eventually, transverse shear and warping) in several works, see for example Yu *et al.* [16, 17]. Nevertheless, the analysis of more complicated problems, such as thin-walled beams subjected to local effects and other higher-order phenomena may require the use of refined beam theories. For example, Genoese *et al.* [18] implemented a geometrically nonlinear model for homogeneous and isotropic beams with generic cross-section by employing a three-dimensional linear elastic model which extends the Saint-Venant solution to non-uniform warping cases. The Generalized Beam Theory (GBT) was extended to the post-buckling analysis of thin-walled steel frames by Basaglia *et al.* [19] by using the finite element method and incorporating the influence of frame joints. Recently, Machado [20] utilized the Ritz method along with the Newton-Raphson linearization scheme to investigate the buckling and post-buckling of thin-walled beams with the aid of a theory which includes bending and warping shear deformability. Also, it is worthy to mention the work of Garcea *et al.* [21], who addressed the geometrically nonlinear analysis of beams and shells using solid finite elements.

Most of the research articles in the literature, including the aforementioned ones, employ the von Kármán nonlinear strain approximation to assess the load-carrying capability of highly flexible structures. Carrera and Parisch [22], in the study of composite shells, demonstrated that von Kármán approximations yield good accuracy in the case of thin elastic structures when deflections are of the same order of magnitude of the thickness. However, the same authors highlighted that such accuracy is not confirmed in the case of thick structures. Furthermore, evidently the error made by von Kármán approximations is higher in the case of shear loadings, where rotations can be considered neither small nor moderate. A few years earlier, in the analysis of laminated cylindrical panels, also Kim and Chaudhuri [23] underlined that the von Kármán strains approximation overestimates the transverse displacements, especially in the advanced nonlinear regime. These remarks can be directly extended to 1D structures. For example, Pacoste and Eriksson [24] investigated different strain formulations for beam elements in instability analysis and also provided an energetic argument to justify why certain strain measures are needed to capture certain nonlinear effects. In this domain, this work wants to investigate the effectiveness of various nonlinear strain assumptions for the analysis of simple 1D to complicated 2D and shell

problems. The investigation is conducted by utilizing the Carrera Unified Formulation (CUF) [25, 26], according to which any theory of structures can degenerate into a generalized kinematics that makes use of an arbitrary expansion of the generalized variables. In other words, the governing equations and the related finite element arrays of beams as well as shells can be written in terms of *fundamental nuclei* for both linear [27, 28] and nonlinear [29, 30] problems. Also, thanks to its intrinsic scalable nature, full to simple von Kármán nonlinear strain approximations can be automatically and opportunely incorporated by using CUF.

The paper is organized as follows: (i) first, a brief discussion about geometrical nonlinear relations is given in Section II; then, (ii) CUF and related nonlinear FE approximation are discussed in Section III to give the fundamental nuclei of the secant and the tangent stiffness matrices accounting for Green-Lagrange to von Kármán strains; (iii) numerical results are presented in Section IV, where attention is focused on post-buckling of solid cross-section beams as well as on large-displacement analysis of thin-walled structures; finally, (iv) the main conclusions are drawn in Section V.

II. Nonlinear geometric relations

When the square of displacement derivatives are finite, as in the case of large displacements and rotations analysis as well as elastic post-buckling, the problem of characterizing the strain tensor from the initial state is not trivial, see [31]. As a matter of fact, reliable nonlinear analyses require accurate definitions of strains and stresses. In pure geometrically nonlinear problems, *Lagrangian* formulations are generally employed because there is a natural undeformed state to which the structure would return if unloaded. In fact, in contrast to *Eulerian* formulation, strains are expressed in terms of the undeformed configuration in the case of Lagrangian approach. This aspect entails a number of advantages when a Lagrangian formulation is utilized along with an implicit numerical incremental solution scheme. [1]. As an example, stress and strain components do not need any coordinate transformation at each iteration. Furthermore, large steps can be used with no loss of accuracy if the implemented method is convergent.

In the domain of total Lagrangian formulations, models employing Green-Lagrange strain measures are well developed in the literature. The reasons are twofold. First, Green-Lagrange strains vanish for rigid body rotations (this is not true in the case of engineering strains). Second, these strains are work-conjugate to second Piola-Kirchoff stresses. Given a three-dimensional displacement field $\mathbf{u}(x, y, z) = \{u_x \ u_y \ u_z\}^T$, (x, y, z) being the Cartesian coordinate system, the Green-Lagrange strain components can be defined as:

$$\boldsymbol{\epsilon} = \boldsymbol{\epsilon}_l + \boldsymbol{\epsilon}_{nl} = (\mathbf{b}_l + \mathbf{b}_{nl})\mathbf{u} \tag{1}$$

where $\boldsymbol{\epsilon} = \{\epsilon_{xx} \ \epsilon_{yy} \ \epsilon_{zz} \ \epsilon_{xz} \ \epsilon_{yz} \ \epsilon_{xy}\}^T$ is the vector of the strain components, and $\mathbf{b}_l$ and $\mathbf{b}_{nl}$ are the linear and nonlinear

differential operators, respectively. They read:

$$
\mathbf{b}_l =
\begin{bmatrix}
\partial_x & 0 & 0 \\
0 & \partial_y & 0 \\
0 & 0 & \partial_z \\
\partial_z & 0 & \partial_x \\
0 & \partial_z & \partial_y \\
\partial_y & \partial_x & 0
\end{bmatrix}
, \qquad
\mathbf{b}_{nl} =
\begin{bmatrix}
\frac{1}{2}(\partial_x)^2 & \frac{1}{2}(\partial_x)^2 & \frac{1}{2}(\partial_x)^2 \\
\frac{1}{2}(\partial_y)^2 & \frac{1}{2}(\partial_y)^2 & \frac{1}{2}(\partial_y)^2 \\
\frac{1}{2}(\partial_z)^2 & \frac{1}{2}(\partial_z)^2 & \frac{1}{2}(\partial_z)^2 \\
\partial_x\,\partial_z & \partial_x\,\partial_z & \partial_x\,\partial_z \\
\partial_y\,\partial_z & \partial_y\,\partial_z & \partial_y\,\partial_z \\
\partial_x\,\partial_y & \partial_x\,\partial_y & \partial_x\,\partial_y
\end{bmatrix}
\tag{2}
$$

where $\partial_x = \dfrac{\partial(\cdot)}{\partial x}$, $\partial_y = \dfrac{\partial(\cdot)}{\partial y}$, and $\partial_z = \dfrac{\partial(\cdot)}{\partial z}$. Note that three rows in Eq. (2) are not strictly speaking the Green-Lagrange shear strains as they have been multiplied by 2 to make them compatible with the typical constitutive relation.

The inclusion of appropriate geometric nonlinearities in large displacements and rotations analysis is of fundamental importance. The reason is that large displacements and rotations may *activate* coupling phenomena among bending, extension, shear and torsion of structures. Equation (2) includes full three-dimensional (3D) Green-Lagrange strains. Over the last decades, on the other hand, many geometric nonlinear models have been developed for two-dimensional (2D) and one-dimensional (1D) structures from simplifications of full 3D relations. A famous example is represented by von Kármán strains for plates, see [32]. In the case of thin flat plates and moderate rotations, von Kármán hypothesizes that the quadratic terms of Eq. (2) that cannot be neglected are those related to the in-plane partial derivatives of the transverse displacements. In essence, the aforementioned non-linear geometric relations for von Kármán strains read:

$$
\begin{aligned}
\epsilon_{xx_{nl}} &= \frac{1}{2}(u_{z,x})^2 \\
\epsilon_{yy_{nl}} &= \frac{1}{2}(u_{z,y})^2 \\
\epsilon_{xy_{nl}} &= u_{z,x}u_{z,y}
\end{aligned}
\tag{3}
$$

In the case of 1D beams and according to von Kármán assumptions, the only non-zero component of the nonlinear strain vector would be:

$$
\epsilon_{yy_{nl}} = \frac{1}{2}(u_{z,y})^2
\tag{4}
$$

In writing Eqs. (3) and (4), notation of Fig. 1 is employed. This figure proposes a qualitative representation of a plate and a beam subjected to large displacements. Note that the *z*-axis is placed along the thickness of the plate, whereas the undeformed beam axis lays along *y*-axis. It is well known that von Kármán strains do not account for moderate rotations [1] though.
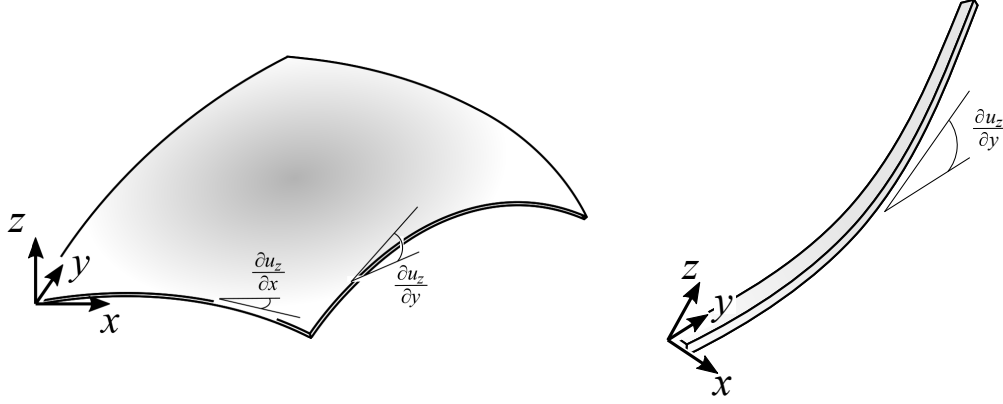
Fig. 1 Flexible plate and beam structures.

The present research work wants to further investigate the effect of different nonlinear strain assumptions in the large displacements/rotations analysis of flexible structures. To address this objective, the Carrera Unified Formulation (CUF) is used. Given the scalable nature of CUF, in fact, the nonlinear governing equations of beam, plate and shell structures can be formulated with ease and in a unified manner. Moreover, geometric relations accounting for full 3D Green-Lagrange strains (Eq. (2)) to von Kármán strains (Eqs. (3) and (4)) can be addressed by eventually nullifying or adding the corresponding nonlinear terms into the CUF fundamental nuclei, which represent the basic building blocks of the secant and tangent stiffness matrices.

III. Adopted refined beam theory

A. CUF and finite element approximation

CUF assumes that the three-dimensional displacement field $\mathbf{u}(x, y, z)$ can be expressed as a general expansion of the primary unknowns. In the case of one-dimensional theories, one has:

$$\mathbf{u}(x, y, z) = F_s(x, z)\mathbf{u}_s(y), \qquad s = 1, 2, ..., M \tag{5}$$

where F_s are the functions of the coordinates x and z on the cross-section, $\mathbf{u}_s$ is the vector of the *generalized* displacements which lay along the beam axis, M stands for the number of the terms used in the expansion, and the repeated subscript s indicates summation. The choice of F_s determines the class of the 1D CUF model that is required and subsequently to be adopted.

In this paper, Lagrange polynomials are used as F_s cross-sectional functions. The resulting beam theories are known as LE (Lagrange Expansion) CUF models in the literature [26]. LE models utilize only pure displacements as primary unknowns and they have been recently used for the component-wise analysis of aerospace and civil engineering constructions as well as for composite laminates and box structures, see [33–38]. Lagrange polynomials as used in

this paper can be found in [39]. In the domain of CUF, linear three- (L3) and four-point (L4), quadratic six- (L6) and nine-point (L9), as well as cubic 16-point (L16) Lagrange polynomials have been used to formulate linear to higher-order kinematics beam models. For a further improvement of the beam kinematics and a geometrically correct (isoparametric) description of complex cross-section beams, a combination of Lagrange polynomials can be used in a straightforward manner by employing CUF. For more details about LE beam theories, the readers are referred to the original paper by Carrera and Petrolo [40].

For the sake of generality, the Finite Element Method (FEM) is adopted to discretize the structure along the y-axis. Thus, the generalized displacement vector $\mathbf{u}_s(y)$ is approximated as follows:

$$\mathbf{u}_s(y) = N_j(y)\mathbf{q}_{sj} \qquad j = 1, 2, \ldots, p+1 \tag{6}$$

where N_j stands for the j-th shape function, p is the order of the shape functions and j indicates summation. $\mathbf{q}_{sj} = \{q_{x_{sj}} \ q_{y_{sj}} \ q_{z_{sj}}\}^T$ is the vector of the FE nodal parameters. For the sake of brevity, the shape functions N_j are not reported here. They can be found in many reference texts, for instance in Bathe [39]. However, it should be underlined that the choice of the cross-section polynomials sets for the LE kinematics (i.e. the selection of the type, the number and the distribution of cross-sectional polynomials) is completely independent of the choice of the beam finite element to be used along the beam axis. In this work, classical one-dimensional finite elements with four nodes (B4) are adopted, i.e. a cubic approximation along the y-axis is assumed.

B. Nonlinear governing equations

According to the principle of virtual work, the sum of the virtual variation of internal strain energy (δL_{int}) and the virtual variation of the work of external loadings (δL_{ext}) must be null for any arbitrary infinitesimal virtual displacement satisfying the prescribed geometrical constraints. In essence,

$$\delta L_{\text{int}} - \delta L_{\text{ext}} = 0 \tag{7}$$

Large deflection analysis of elastic systems results in complex nonlinear differential problems. Nevertheless, the equilibrium condition of the structure can be expressed as a system of nonlinear algebraic equations if FEM and CUF are utilized.

The virtual variation of the strain energy, for example, can be expressed as

$$\delta L_{\text{int}} = <\delta\boldsymbol{\epsilon}^T \boldsymbol{\sigma}> \tag{8}$$

where $<(\cdot)> = \int_V (\cdot) \, dV$ and $\boldsymbol{\sigma}$ is the stress vector. Under the hypothesis of small deformations, $V = \Omega \times L$ is the initial

volume of the beam structure. The strain vector ϵ in Eq. (1) can be written in terms of the generalized nodal unknowns $\mathbf{q}_{sj}$ by employing Eqs. (5) and (6).

$$\epsilon = (\mathbf{B}_l^{sj} + \mathbf{B}_{nl}^{sj})\mathbf{q}_{sj} \tag{9}$$

where $\mathbf{B}_l^{sj}$ and $\mathbf{B}_{nl}^{sj}$ are the two following matrices:

$$\mathbf{B}_l^{sj} = \mathbf{b}_l(F_s N_j) = \begin{bmatrix} F_{s,x} N_j & 0 & 0 \\ 0 & F_s N_{j,y} & 0 \\ 0 & 0 & F_{s,z} N_j \\ F_{s,z} N_j & 0 & F_{s,x} N_j \\ 0 & F_{s,z} N_j & F_s N_{j,y} \\ F_s N_{j,y} & F_{s,x} N_j & 0 \end{bmatrix} \tag{10}$$

and

$$\mathbf{B}_{nl}^{sj} = \frac{1}{2} \begin{bmatrix} u_{x,x} F_{s,x} N_j & u_{y,x} F_{s,x} N_j & u_{z,x} F_{s,x} N_j \\ u_{x,y} F_s N_{j,y} & u_{y,y} F_s N_{j,y} & u_{z,y} F_s N_{j,y} \\ u_{x,z} F_{s,z} N_j & u_{y,z} F_{s,z} N_j & u_{z,z} F_{s,z} N_j \\ u_{x,x} F_{s,z} N_j + u_{x,z} F_{s,x} N_j & u_{y,x} F_{s,z} N_j + u_{y,z} F_{s,x} N_j & u_{z,x} F_{s,z} N_j + u_{z,z} F_{s,x} N_j \\ u_{x,y} F_{s,z} N_j + u_{x,z} F_s N_{j,y} & u_{y,y} F_{s,z} N_j + u_{y,z} F_s N_{j,y} & u_{z,y} F_{s,z} N_j + u_{z,z} F_s N_{j,y} \\ u_{x,x} F_s N_{j,y} + u_{x,y} F_{s,x} N_j & u_{y,x} F_s N_{j,y} + u_{y,y} F_{s,x} N_j & u_{z,x} F_s N_{j,y} + u_{z,y} F_{s,x} N_j \end{bmatrix} \tag{11}$$

In Eqs. (10) and (11), commas denote partial derivatives. Note that Eq. (11) is valid for the full 3D Green-Lagrange strains of Eq. (2). It can be easily modified to account for different geometric nonlinearities assumptions. For example, in the case of von Kármán strains of Eq. (4), the nonlinear (but algebraic) geometric operator would hold

$$\mathbf{B}_{nl}^{sj^{1DVK}} = \frac{1}{2} \begin{bmatrix} 0 & 0 & 0 \\ 0 & 0 & u_{z,y} F_s N_{j,y} \\ 0 & 0 & 0 \\ 0 & 0 & 0 \\ 0 & 0 & 0 \\ 0 & 0 & 0 \end{bmatrix} \tag{12}$$

If these geometric relations are substituted into Eq. (8) along with the Hooke's law and CUF (Eqs. (5) and (6)), one has:

$$\delta L_{\text{int}} = \delta \mathbf{q}_{\tau i}^T < \left(\mathbf{B}_l^{\tau i} + 2 \mathbf{B}_{nl}^{\tau i} \right)^T \mathbf{C} \left(\mathbf{B}_l^{sj} + \mathbf{B}_{nl}^{sj} \right) > \mathbf{q}_{sj} = \delta \mathbf{q}_{\tau i}^T \mathbf{K}_S^{ij\tau s} \mathbf{q}_{sj} \tag{13}$$

where τ and i are the CUF summation indexes over the variations' primary unknowns (i.e., $\delta \mathbf{u}(x, y, z) = F_\tau(x, z) N_i(y) \mathbf{q}_{\tau i}$); $\mathbf{C}$ is the matrix of the material elastic coefficients; $\mathbf{B}_l^{\tau i}$ is the matrix of the linear geometric relations; $\mathbf{B}_{nl}^{\tau i}$ is the matrix of the nonlinear geometric relations (Eqs. (11) or (12) or any variation of thereof); and $\mathbf{K}_S^{ij\tau s}$ is the *Fundamental Nucleus* (FN) of the *secant* stiffness matrix. Note that, in Eq. (13), we take for granted that $\delta \boldsymbol{\epsilon} = (\mathbf{B}_l^{\tau i} + 2 \mathbf{B}_{nl}^{\tau i}) \delta \mathbf{q}_{\tau i}$. The FN of the secant stiffness matrix is not given here for the sake of brevity. However, the formal calculation of $\mathbf{K}_S^{ij\tau s}$ can be found in the work of Pagani and Carrera [29]. It is a 3×3 matrix that, given the cross-sectional functions ($F_\tau = F_s$, for $\tau = s$) and the shape functions ($N_i = N_j$, for $i = j$), can be expanded by using the indexes $\tau, s = 1, ..., M$ and $i, j = 1, ..., p + 1$ in order to obtain the elemental secant stiffness matrix of any arbitrarily refined beam model. In other words, by opportunely choosing the beam kinematics (i.e., by choosing F_τ as well as the number of expansion terms M) classical to higher-order beam theories and related secant stiffness arrays can be implemented in an automatic manner by exploiting the index notation of CUF. Moreover, it is evident that $\mathbf{K}_S^{ij\tau s}$ can be modified to contain different geometrical nonlinear approximations, from full 3D Green-Lagrange strains of Eq. (2) to simple von Kármán strains of Eq. (4), by opportunely varying $\mathbf{B}_{nl}^{\tau i}$. Once the elemental secant stiffness matrix is obtained according to the desirable approximation order and for the generic nonlinear strains approximation, it can be assembled as conventional FEM [26].

The nonlinear algebraic governing equations can be, thus, obtained from Eq. (7) after the virtual variation of the external work is also formalized (conservative problems are addressed in this work).

$$\mathbf{K}_S \mathbf{q} - \mathbf{p} = 0 \tag{14}$$

where $\mathbf{K}_S$, $\mathbf{q}$, and $\mathbf{p}$ are global, assembled finite element arrays of the final structure. For more details about the calculation of the work of external loadings and the related vector of generalized forces $\mathbf{p}$, interested readers are referred to Carrera *et al.* [26].

C. Linearization

Equation (14) constitutes the starting point for finite element calculation of geometrically nonlinear systems, and it is usually solved through an incremental linearized scheme, typically the Newton-Raphson method (or *tangent method*). According to the Newton-Raphson method, the governing equations are written as:

$$\boldsymbol{\varphi}_{res} \equiv \mathbf{K}_S \mathbf{q} - \mathbf{p} = 0 \tag{15}$$

9

where $\boldsymbol{\varphi}_{res}$ is the vector of the *residual nodal forces* (unbalanced nodal force vector). Equation (15) can now be linearized by expanding $\boldsymbol{\varphi}_{res}$ in Taylor's series about a known solution $(\mathbf{q}, \mathbf{p})$. Omitting the second-order terms, one has

$$\boldsymbol{\varphi}_{res}(\mathbf{q} + \delta\mathbf{q}, \mathbf{p} + \delta\mathbf{p}) = \boldsymbol{\varphi}_{res}(\mathbf{q}, \mathbf{p}) + \frac{\partial\boldsymbol{\varphi}_{res}}{\partial\mathbf{q}} \delta\mathbf{q} + \frac{\partial\boldsymbol{\varphi}_{res}}{\partial\mathbf{p}} \delta\lambda \, \mathbf{p}_{ref} = 0 \tag{16}$$

where $\dfrac{\partial\boldsymbol{\varphi}_{res}}{\partial\mathbf{q}} = \mathbf{K}_T$ is the *tangent* stiffness matrix, and $-\dfrac{\partial\boldsymbol{\varphi}_{res}}{\partial\mathbf{p}}$ is equal to the unit matrix $\mathbf{I}$. In Eq. (16) it has been assumed that the load varies directly with the vector of the reference loadings $\mathbf{p}_{ref}$ and has a rate of change equal to the load parameter λ, i.e. $\mathbf{p} = \lambda \, \mathbf{p}_{ref}$. Also, note that, as the load-scaling parameter λ is taken as a variable, an additional governing equation is required to Eq. (16) and this is given by a constraint relationship $c(\delta\mathbf{q}, \delta\lambda)$ to finally give

$$\begin{cases} \mathbf{K}_T \, \delta\mathbf{q} = \delta\lambda \, \mathbf{p}_{ref} - \boldsymbol{\varphi}_{res} \\ \\ \\ c(\delta\mathbf{q}, \delta\lambda) = 0 \end{cases} \tag{17}$$

Depending on the constraint equation, different incremental schemes can be implemented. For example, if the constraint equation is $\delta\lambda = 0$, Eq. (17) corresponds to a load-control method. On the other hand, the condition $c(\delta\mathbf{q}, \delta\lambda) = \delta\mathbf{q} = 0$ represents a displacement-control method. In this paper, a path-following method is employed in which the constraint equation is a function of both displacement and load parameter variations. In detail, an arch-length method as proposed by Crisfield [41, 42] and later modified by Carrera [43] is utilized in this work.

For completeness reasons, it is important to underline that the tangent stiffness matrix is derived from the linearization of the equilibrium equations [44]. This corresponds to linearizing the virtual variation of the strain energy in the case of conservative problems:

$$\delta(\delta L_{\text{int}}) = < \delta(\delta\boldsymbol{\epsilon}^T \boldsymbol{\sigma}) > = \delta\mathbf{q}_{\tau i}^T \mathbf{K}_T^{ij\tau s} \delta\mathbf{q}_{sj} \tag{18}$$

As in the case of the secant matrix, $\mathbf{K}_T^{ij\tau s}$ represents the 3×3 FN and it is the basic building block to be used for the formulation of the tangent stiffness matrix for any higher-order refined beam elements accounting for Green-Lagrange nonlinear strains or any other nonlinear strains approximation. The detailed formulation of the tangent matrix is not straightforward and is not given in this paper. Nonetheless, a comprehensive formulation of the geometrical nonlinear problem in the domain of CUF is provided in the work of Pagani and Carrera [29].
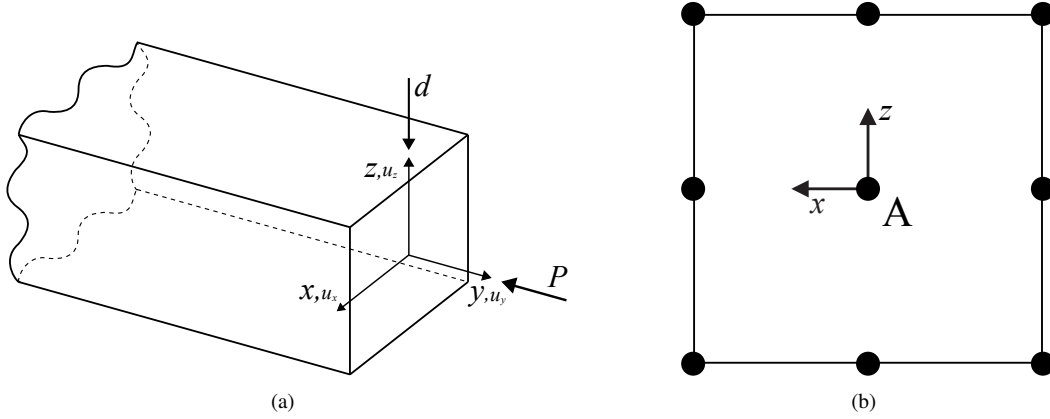
Fig. 2 **Reference system and displacement notation (a) and cross-section discretization (b) for the square cross-section beam.**

IV. Numerical results

A. Post-buckling of square cross-section beam

In the first analysis case, a cantilever beam with a square cross-section is considered. The beam is made of an aluminum alloy with Young modulus E equal to 75 GPa and Poisson ratio $\nu = 0.33$. The aspect-ratio ratio L/w is equal to 100, where L is the beam length and w is the side width. The loading condition is depicted in Fig. 2(a) and involves an axial load P to investigate buckling and post-buckling behavior of the structure, and a small load defect d at the free end of the beam to *activate* the stable branch along the nonlinear path. The load defect d is equal to 0.2% of the critical buckling load. Also, according to Pagani and Carrera [29], quadratic kinematics describes well the post-buckling behavior for the problem addressed. Thus, one single L9 Lagrange polynomial was used to approximate the displacement field, see Fig. 2(b). On the other hand, 20 cubic beam elements are used along the longitudinal axis.

Results of the proposed static response analysis are depicted in Fig. 3. Different analyses are considered and they differ in the approximation of the nonlinear geometrical relations. In essence, each analysis makes use of a different operator $\mathbf{b}_{nl}$. Each curve of Fig. 3 is marked by a number, which refers to a specific set of nonlinear parameters specified by the respective matrix, shown in the top left of the figure. Black dots denote the nonlinear terms of matrix $\mathbf{b}_{nl}$ which are active in the current analysis. For instance, the first matrix corresponds to the nonlinear analysis with all parameters involved (i.e., full Green-Lagrange strains are considered). On the contrary, case number 4 denotes a linear analysis. Results of analysis case number 1 show that nonlinearities in the x (or u) direction have no influence in the overall behavior of the structure. The analysis case number 2 in Fig. 3 utilizes the von Kármán assumptions to 1D beams, presented in Section II. This nonlinear matrix produces an almost horizontal line after the buckling load is reached and it varies from the full nonlinear solution around the displacement value of 0.2. It is important to notice that higher-order models including shear effects are employed in this work. This means that translational and rotary mechanics are

11

decoupled in the present beam analysis. Thus, one must include nonlinear effects on shear strains along with bending in order to fulfill the compatibility between the von Kármán strains and the model kinematics (analysis number 3 in Fig. 3, where both $1/2 \left(\partial_y u_z \right)^2$ and $1/2 \left(\partial_z u_y \right)^2$ are included). Similar considerations can be drawn by energetic analysis, see for example the work of Pacoste and Eriksson [24]. In the final analysis, the fifth curve has the purpose to show how the solution can change if different nonlinear parameters are chosen. From the third matrix of the first analysis, $\frac{\partial u_z}{\partial z}$ is neglected from the nonlinear strain tensor: the result shows a trend more similar to the full nonlinear solution until the displacement reaches the value of 0.4. Table 1 shows the different values of loads for the first, third, fourth, fifth and sixth cases for three levels of u_z/L.
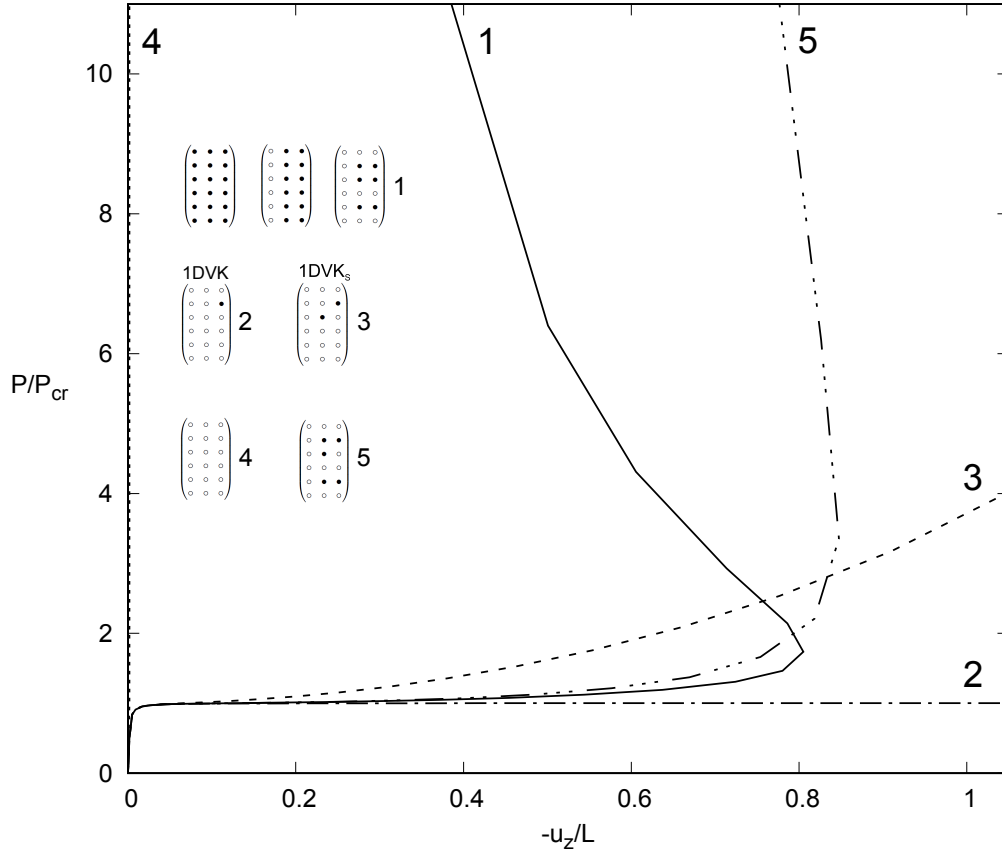
Fig. 3   Equilibrium curves of the cantilever beam subjected to compression and for various geometrical nonlinear approximations. $P_{cr} = \frac{4L^2}{\pi^2 EI}$

B. Bending and twisting of a thin-walled beam

The second analysis case concerns a cantilever thin-walled beam. The material properties are the same as in the first analysis case. The geometry of the cross-section is described in Fig. 4(a), and the aspect ratio L/h is equal to 20, and $L/w = 5$. A vertical load P is acting at the corner of the section of the beam, as shown in Fig. 4. The employed beam model utilizes a quadratic kinematics ($1L9$ on the cross-section) and $20B4$ elements along the beam axis.

Table 1 **Representative equilibrium states of the cantilever beam in post-buckling and for various geometrical nonlinear approximations.** *P* **is expressed in kN.**

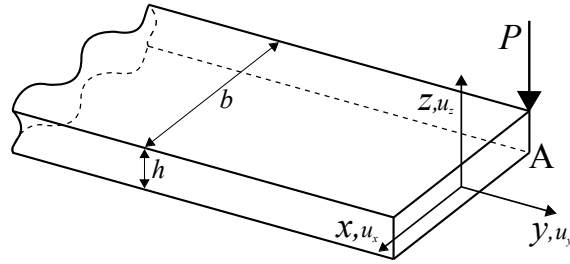| $-u_{zA}/L$	P		
0.2	61.42	63.58	61.61
0.4	62.38	67.62	62.43
0.6	63.70	76.27	64.24

Fig. 4   Rectangular cross-section beam subjected to flexure and torsion.

Fig. 5 shows equilibrium curves (transverse displacements at point A vs. load P) for various strain assumptions. Analysis number 1 in Fig. 5 makes use of the full nonlinear Green-Lagrange strain tensor. The first analysis also demonstrates that neglecting the higher-order derivatives of the displacement component u_x (first column of the matrix $\mathbf{b}_{nl}$) does not affect the accuracy of the solution. Contrary to the results of the previous case, the derivatives along the x coordinate have some influence on the results. In fact, the second analysis leads to a slightly different curve than the previous two, being a less conservative solution than the full nonlinear case; the nonlinearities due to cross-sectional deformation needs to be included because the beam is subjected to torsion. Analysis number 3 in Fig. 5 shows that classical Kármán approximations lead to linear solution, despite the nonlinear terms. As in the previous analysis case, and because the proposed model inherently incorporates shear effects, the nonlinear strain tensor must include both $1/2 \left(\partial_y u_z\right)^2$ and $1/2 \left(\partial_z u_y\right)^2$ to satisfy consistency requirements. This has been done in the fourth and fifth analyses, which lead to solutions that are similar to the full nonlinear solution, with the 2D von Kármán being closer. Analysis number 6 in Fig. 5 shows another nonlinear approximation, which is less conservative during the overall analysis. Some of the most relevant deformed configurations are depicted in Fig. 5 to show the differences of the proposed solutions, and Tables 2 and 3 show the shapes for all the curves in two planes, for the displacement near to $u = 1$ m.
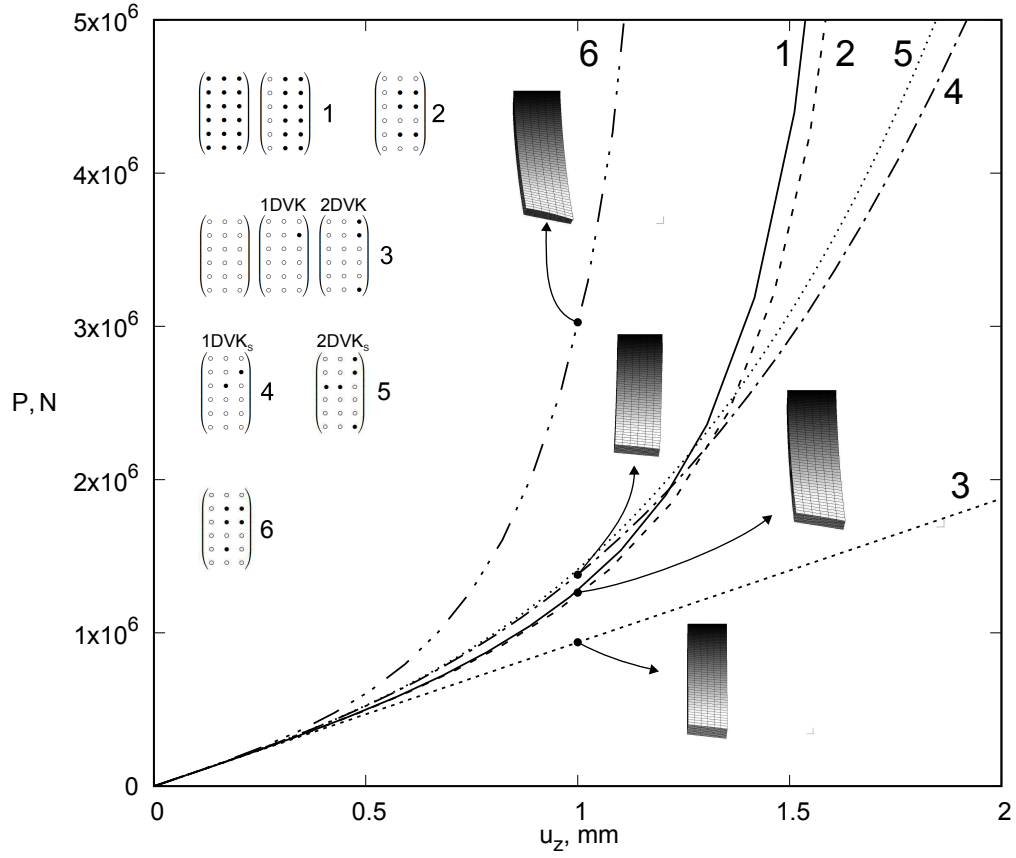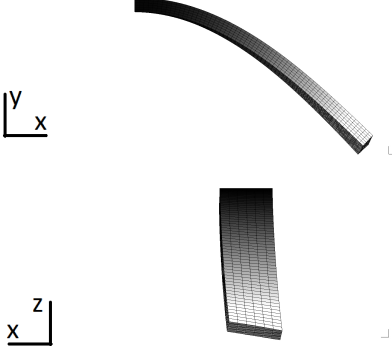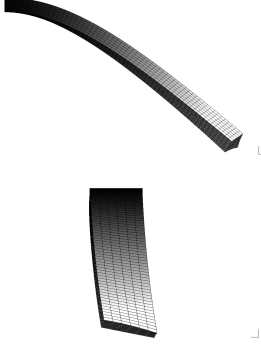
Fig. 5   Equilibrium curves of the cantilever rectangular beam subjected to flexure and torsion.

Table 2   Deformed configurations of the cantilever rectangular cross-section beam for nonlinear relations 1, 2, and 3.

| $u_z = 0.982$ m | $u_z = 1.075$ m | $u_z = 1.07$ m |
| $P = 0.124 \times 10^7$ N | $P = 0.141 \times 10^7$ N | $P = 0.1 \times 10^7$ N |

Table 3 Deformed configurations of the cantilever rectangular cross-section beam for nonlinear relations 4, and 6.

$u_z = 1.041$ m	$u_z = 1.024$ m
$P = 0.147 \times 10^7$ N	$P = 0.329 \times 10^7$ N

C. Thin-walled unsymmetric beam

This section focusses on a cantilever unsymmetric channel section beam, which geometry is shown in Fig. 6(a) and has $b = 100$ mm, $h_1 = 48$ mm, $h_2 = 40$ mm and $t = 10$ mm. The length of the beam is $L = 1$ m. The material properties are the same as in the previous cases. In Fig. 6, the loading condition is also depicted, and a P load is acting in the mid-span of the upper side in the z direction. The 7L9 polynomial set has been employed to approximate the beam kinematics on the cross-section, see Fig. 6(b), and 20 cubic elements are used to discretize the beam axis. Some analyses have been conducted to investigate the effects that the parameters of the nonlinear matrix $\mathbf{b}_{nl}$ have on the static solution of the problem, and equilibrium curves are shown in Fig. 6(b), which gives the evolution of transverse displacement at point A against applied load P.

The full nonlinear solution has been highlighted in Fig. 7 and it corresponds to the first analysis, where all the spots in the $\mathbf{b}_{nl}$ matrix are black. In this analysis case, quadratic terms of the derivatives of the displacement component u_x have a strong influence. The curves from the second analysis is completely different from the first one, due to the fact that the beam is subjected to coupled bending and torsion. As a matter of fact, the torsion suggests that the nonlinear strains coming from large u_x displacements are of fundamental importance in this analysis case.

Curve of analysis number 4 in Fig. 7 shows the solution from classical 1D von Kármán approximation. Again, analysis number 5 suggests the importance to include shear terms. This solution is comparable with the nonlinear solution from case IV.B, because we are dealing with this case as it is a 1D problem, neglecting all local effects that may occur in cross-section, especially near the clamped side. The same discussion can be extended to 2D von Kármán
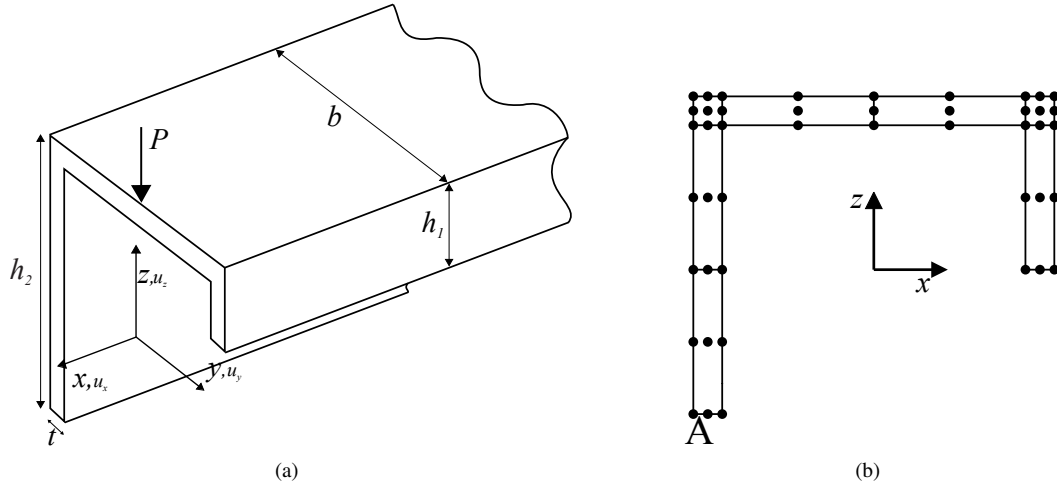
Fig. 6 Reference system and displacement notation (a) and cros-section discretization (b) for the thin-walled unsymmetric cross-section beam.
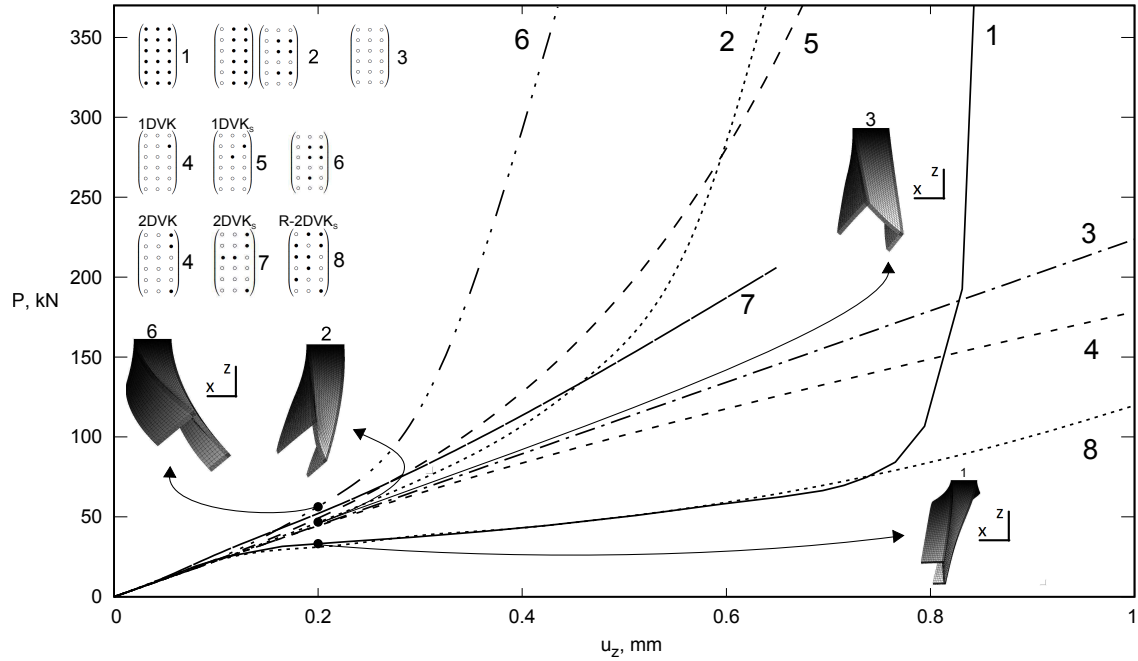

Fig. 7 Equilibrium curves of the cantilever thin-walled unsymmetric beam subjected to flexure and for various geometrical nonlinear approximations.

approximation, but to reproduce the right curve, it is not enough to include the same terms which have been included in the example IV.B for the curve 5. In fact, approximations 4 and 7 in Fig. 7 lead to curves that completely differs from the nonlinear analysis. It is necessary to take into account the rotation of the cross-section depicted in Fig. 6 and this leads to the set of nonlinear parameters of the matrix 8. The curve associated follows with an high accuracy the full nonlinear solution until the displacement reaches the value of 0.7 mm. Then, the displacement for the 2D von Kármán theory keeps increasing, while the full nonlinear solution describes a structure with greater stiffness. Curve 6 represents another nonlinear solution, which is less conservative from the other nonlinear sets.

D. Pinched thin-walled cylinder

The final result analysis case concerns a pinched cylinder. Material and geometrical data comes from Flügge [45]. The material is isotropic with Young modulus $E = 3 \times 10^6$ psi and Poisson ratio $v = 0.3$. The geometry is shown in Fig. 8(a), with length $L = 600$ in, radius $r = 300$ in and thickness $t = 3$ in. The displacement field over the cross-section has been evaluated through 30L16 Lagrange polynomials, because in Carrera *et al* [46] has been shown that this kind of theory can describe with accuracy the displacements of the structure. The method adopted can be seen in Fig. 8(b), and the elements over the cross-section have been distributed linearly in order to refine the discretization in proximity to the loading point (so that $A_1/A_2 = 10$).
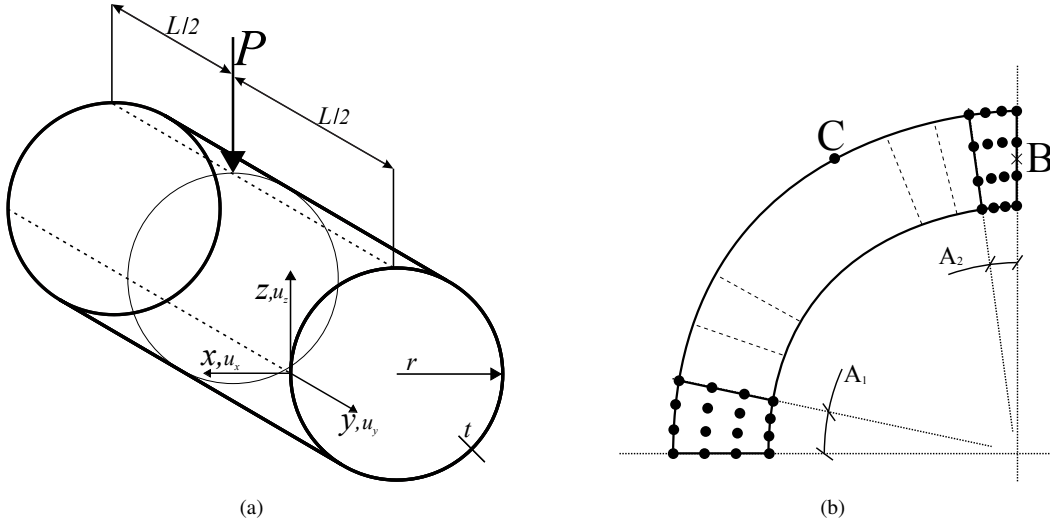

(a)   (b)

Fig. 8   Reference system and displacement notation (a) and cros-section discretization (b) for the thin-walled pinched cylinder.

Figure 9 shows the trends of the z component of the displacement of the B point (Fig. 8(b)) for different kinds of nonlinear analyses. The first curve corresponds to the full nonlinear analysis, and it is shown that the same result can also be obtained neglecting the first *or* the second column of the nonlinear matrix $\mathbf{b}_{nl}$. Curve 2 represents the linear solution, as this analysis does not include any nonlinear term. Solutions 3 and 4 represent two different sets of nonlinear

17

parameters, which lead to a shallow curve with high displacements at low loadings, and to a curve very close to the linear one, respectively. Regarding the von Kármán theories, curves 5 and 7 represent the solution for the traditional 1D and 2D sets of approximations, with the 2D one being very close to the nonlinear one. It is interesting to note that including or not other nonlinear terms to adapt the von Kármán approximations to the higher-order kinematic theory (as it has been done in the previous analyses cases) leads to the same static solution (for the 2D instance, the solution is the same, while for the 1D solution the difference - between curve 5 and 6 - is slight), which is a consequence of the 3D nature of the problem under consideration. In Fig. 9 some deformations are also depicted. For the same analysis case, Fig. 10 shows the transverse displacement of the point C. From this figure, similar conclusions can be drawn. Tables 4 and 5 finally show some values of the displacement of the two points analyzed for the cases studied (each value is obtained by a linear interpolation between two nearest nonlinear steps solution, due to the fact that an arc-length method has been utilized to evaluate the nonlinear behavior of the structure).
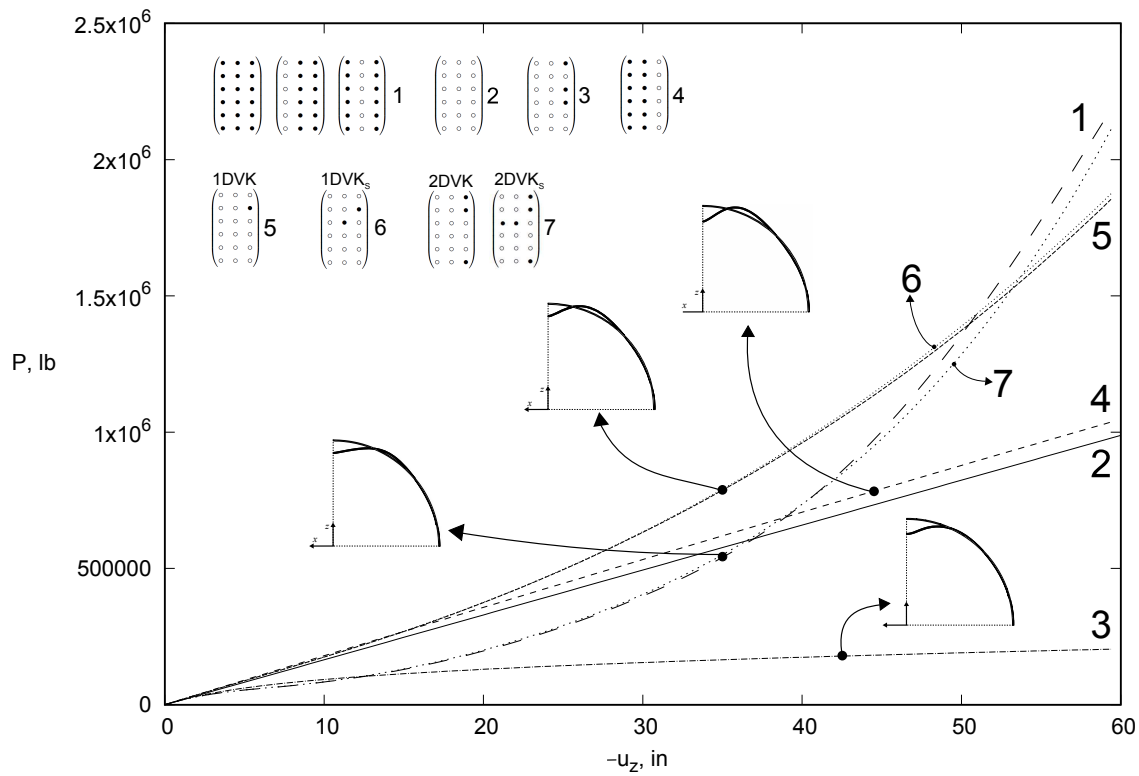

Fig. 9 Equilibrium curves evaluated at point B of the pinched thin-walled cylinder and for various geometrical nonlinear approximations.
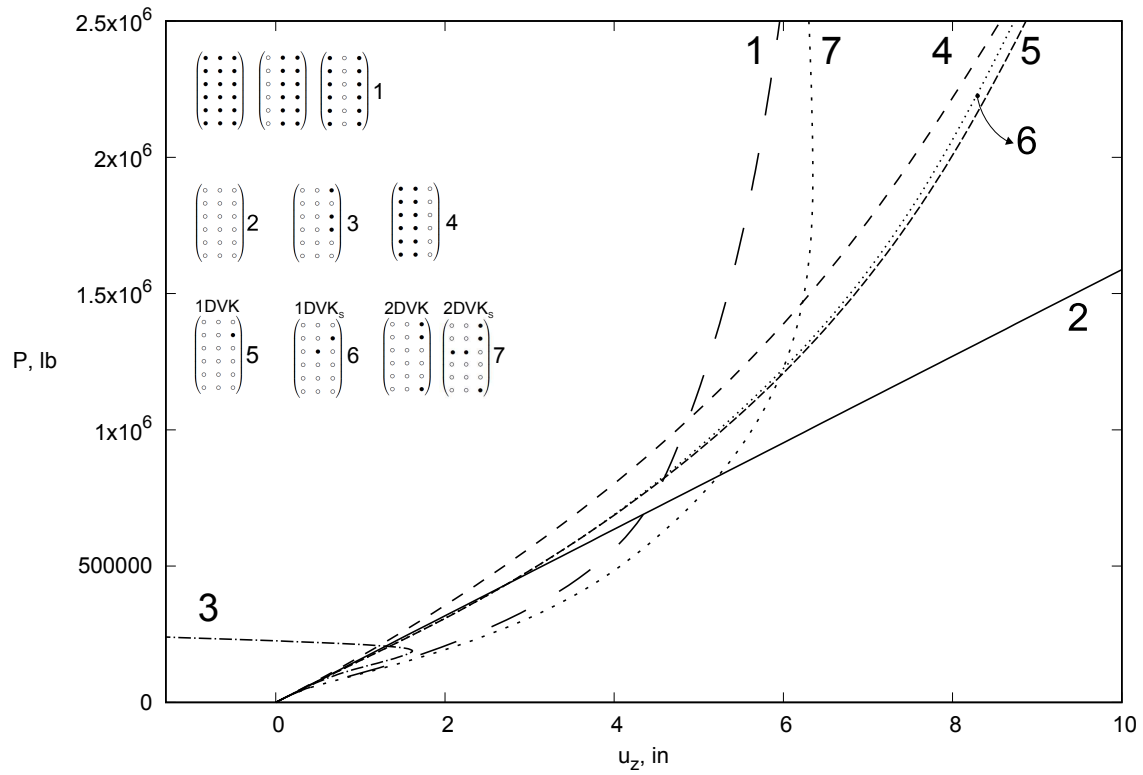
18

Fig. 10 Equilibrium curves evaluated at point C of the pinched thin-walled cylinder and for various geometrical nonlinear approximations.

Table 4 Representative equilibrium states of the pinched thin-walled cylinder and for various geometrical nonlinear approximations. P is expressed in lb $\times 10^3$, u in inches.

P	$-u_{zB}$	$-u_{zB}$	$-u_{zB}$	$-u_{zB}$	$-u_{zB}$
250.0	22.83	15.18	22.91	13.98	-
750.0	39.10	45.53	38.37	42.56	-
1800	54.03	109.3	54.86	108.3	-

19

Table 5 **Representative equilibrium states of the pinched thin-walled cylinder and for various geometrical nonlinear approximations. Values of u_{zC} are shown. P is expressed in lb $\times 10^3$, u in inches.**

P	u_{zC}	u_{zC}	u_{zC}	u_{zC}	u_{zC}
250.0	2.304	1.575	2.530	1.424	-
750.0	4.247	4.724	4.603	3.775	-
1800	5.378	11.34	6.020	6.978	-

V. Conclusions

The present study introduces a refined beam formulation with scalable nature, able to provide classical beam results with von Kármán strains approximation to full nonlinear 3D solutions. In fact, by using the principle of virtual work along with the Carrera Unified Formulation (CUF), the nonlinear governing equations and the related finite element approximation have been expressed in terms of few *fundamental nuclei*, which are independent of the theory approximation order and the strain measurements to be adopted.

The resulting methodology has been employed to investigate the consistency of various geometrical nonlinear strain measurements, without changing its mathematical formalism and in a unified scenario. Several sets of nonlinear terms have been analyzed, including the well known 1D and 2D von Kármán approximations. As general recommendations for the geometrical nonlinear analyses of solid and thin-walled structures, it has been further demonstrated that:

1) The proposed method, based on CUF, represents a tool for comparing different kinematics and strains assumptions in an automatic and efficient way.

2) The geometrical nonlinear relations must be consistent with the kinematics of the theory of structure employed.

3) As known from the previous literature, simplifications of the full Green-Lagrange strain tensor are feasible and may provide acceptable results in the regimes of small and moderate displacements/rotations.

4) von Kármán approximations can be used for the analysis of slender beams under flexure, column buckling initiation, and pinched cylinders. On the other hand, they are discouraged for the analysis of thin-walled beams subjected to bending-torsion-shear couplings.

References

[1] Pai, P. F., *Highly Flexible Structures: Modeling, Computation, and Experimentation*, 2007.

[2] Euler, L., *De curvis elasticis*, Lausanne and Geneva: Bousquet, 1744.

[3] Timoshenko, S. P., and Gere, J. M., *Theory of elastic stability*, Tokyo, 1961.

[4] Bisshopp, K. E., and Drucker, D. C., "Large deflection of cantilever beams," *Quarterly of Applied Mathematics*, Vol. 3, No. 3, 1945, pp. 272–275. doi:10.1090/qam/13360.

[5] Sze, K. Y., Liu, X. H., and Lo, S. H., "Popular benchmark problems for geometric nonlinear analysis of shells," *Finite Elements in Analysis and Design*, Vol. 40, 2004, pp. 1551–1569. doi:10.1016/j.finel.2003.11.001.

[6] Ovesy, H. R., GhannadPour, S. A. M., and Morada, G., "Post-buckling behavior of composite laminated plates under end shortening and pressure loading, using two versions of finite strip method," *Composite Structures*, Vol. 75, No. 1-4, 2006, pp. 106–113.

[7] Milazzo, A., and Oliveri, V., "Buckling and postbuckling of stiffened composite panels with cracks and delaminations by Ritz approach," *AIAA Journal*, Vol. 55, No. 3, 2016, pp. 965–980. doi:10.2514/1.J055159.

[8] Ma, L. S., and Wang, T. J., "Nonlinear bending and post-buckling of a functionally graded circular plate under mechanical and thermal loadings," *International Journal of Solids and Structures*, Vol. 40, No. 13-14, 2003, pp. 3311–3330. doi:10.1016/S0020-7683(03)00118-5.

[9] Arciniega, R. A., Goncalves, P. B., and Reddy, J. N., "Buckling and postbuckling analysis of laminated cylindrical shells using the third-order shear deformation theory," *International Journal of Structural Stability and Dynamics*, Vol. 4, No. 03, 2004, pp. 293–312. doi:10.1142/S0219455404001240.

[10] Arciniega, R. A., and Reddy, J. N., "Large deformation analysis of functionally graded shells," *International Journal of Solids and Structures*, Vol. 44, No. 6, 2007, pp. 2036–2052. doi:10.1016/j.ijsolstr.2006.08.035.

[11] Ko, Y., Lee, P.-S., and Bathe, K.-J., "The MITC4+ shell element in geometric nonlinear analysis," *Computers & Structures*, Vol. 185, 2017, pp. 1–14. doi:10.1016/j.compstruc.2017.01.015.

[12] Timoshenko, S. P., "On the transverse vibrations of bars of uniform cross section," *Philosophical Magazine*, Vol. 43, 1922, pp. 125–131.

[13] Pai, P. F., and Palazotto, A. N., "Large-deformation analysis of flexible beams," *International Journal of Solids and Structures*, Vol. 33, No. 9, 1996, pp. 1335–1353. doi:10.1016/0020-7683(95)00090-9.

[14] Gruttmann, F., Sauer, R., and Wagner, W., "A geometrical nonlinear eccentric 3D-beam element with arbitrary cross-sections," *Computer Methods in Applied Mechanics and Engineering*, Vol. 160, No. 3, 1998, pp. 383–400. doi:10.1016/S0045-7825(97)00305-8.

[15] Mohyeddin, A., and Fereidoon, A., "An analytical solution for the large deflection problem of Timoshenko beams under three-point bending," *International Journal of Mechanical Sciences*, Vol. 78, 2014, pp. 135–139. doi:10.1016/j.ijmecsci.2013.11.005.

[16] Yu, W., Volovoi, V. V., Hodges, D. H., and Hong, X., "Validation of the variational asymptotic beam sectional analysis (VABS)," *AIAA Journal*, Vol. 40, 2002, pp. 2105–2113. doi:10.2514/2.1545.

[17] Yu, W., Hodges, D. H., Volovoi, V. V., and Fuchs, E. D., "A generalized Vlasov theory for composite beams," *Thin-Walled Structures*, Vol. 43, No. 9, 2005, pp. 1493–1511. doi:10.1016/j.tws.2005.02.003.

[18] Genoese, A., Genoese, A., Bilotta, A., and Garcea, G., "A geometrically exact beam model with non-uniform warping coherently derived from the Saint Venant rod," *Engineering Structures*, Vol. 68, 2014, pp. 33–46. doi:10.1016/j.engstruct.2014.02.024.

[19] Basaglia, C., Camotim, D., and Silvestre, N., "Post-buckling analysis of thin-walled steel frames using generalised beam theory (GBT)," *Thin-Walled Structures*, Vol. 62, 2013, pp. 229–242. doi:10.1016/j.tws.2012.07.003.

[20] Machado, S. P., "Non-linear buckling and postbuckling behavior of thin-walled beams considering shear deformation," *International Journal of Non-Linear Mechanics*, Vol. 43, No. 5, 2008, pp. 345–365. doi:10.1016/j.ijnonlinmec.2007.12.019.

[21] Garcea, G., Leonetti, L., and Magisano, D., "Advantages of the mixed format in geometrically nonlinear analysis of beams and shells using solid finite elements," *International Journal for Numerical Methods in Engineering*, 2016. doi:10.1002/nme.5322.

[22] Carrera, E., and Parisch, H., "An evaluation of geometrical nonlinear effects of thin and moderately thick multilayered composite shells," *Composite Structures*, Vol. 40, No. 1, 1997, pp. 11–24.

[23] Kim, D., and Chaudhuri, R. A., "Full and von Karman geometrically nonlinear analyses of laminated cylindrical panels," *AIAA journal*, Vol. 33, No. 11, 1995, pp. 2173–2181. doi:10.2514/3.12963.

[24] Pacoste, C., and Eriksson, A., "Beam elements in instability problems," *Computer Methods in Applied Mechanics and Engineering*, Vol. 144, No. 1–2, 1997, pp. 163–197. doi:10.1016/S0045-7825(96)01165-6.

[25] Carrera, E., Giunta, G., and Petrolo, M., *Beam Structures: Classical and Advanced Theories*, John Wiley & Sons, 2011. doi:10.1002/9781119978565.

[26] Carrera, E., Cinefra, M., Petrolo, M., and Zappino, E., *Finite Element Analysis of Structures through Unified Formulation*, John Wiley & Sons, Chichester, West Sussex, UK, 2014.

[27] Carrera, E., Pagani, A., Petrolo, M., and Zappino, E., "Recent developments on refined theories for beams with applications," *Mechanical Engineering Reviews*, Vol. 2, No. 2, 2015, pp. 1–30. doi:10.1299/mer.14-00298.

[28] Cinefra, M., "Free-vibration analysis of laminated shells via refined MITC9 elements," *Mechanics of Advanced Materials and Structures*, Vol. 23, No. 9, 2016, pp. 937–947. doi:10.1080/15376494.2015.1121556.

[29] Pagani, A., and Carrera, E., "Unified formulation of geometrically nonlinear refined beam theories," *Mechanics of Advanced Materials and Structures*, Vol. 25, No. 1, 2018, pp. 15–31. doi:10.1080/15376494.2016.1232458.

[30] Pagani, A., and Carrera, E., "Large-deflection and post-buckling analyses of laminated composite beams by Carrera Unified Formulation," *Composite Structures*, Vol. 170, 2017, pp. 40–52. doi:10.1016/j.compstruct.2017.03.008.

[31] Malvern, L. E., *Introduction to the Mechanics of a Continuous Medium*, Monograph, 1969.

[32] Gol'Denveizer, A. L., *Theory of Elastic Thin Shells. Solid and Structural Mechanics*, Pergamon Press, 1961.

[33] Carrera, E., Pagani, A., and Petrolo, M., "Classical, Refined and Component-wise Theories for Static Analysis of Reinforced-Shell Wing Structures," *AIAA Journal*, Vol. 51, No. 5, 2013, pp. 1255–1268. doi:10.2514/1.J052331.

[34] Carrera, E., and Pagani, A., "Accurate response of wing structures to free vibration, load factors and non-structural masses," *AIAA Journal*, Vol. 54, No. 1, 2016, pp. 227–241. doi:10.2514/1.J054164.

[35] Carrera, E., Pagani, A., and Petrolo, M., "Refined 1D Finite Elements for the Analysis of Secondary, Primary, and Complete Civil Engineering Structures," *Journal of Structural Engineering*, Vol. 141, 2015, pp. 04014123/1–14. doi: 10.1061/(ASCE)ST.1943-541X.0001076.

[36] Carrera, E., and Pagani, A., "Free vibration analysis of civil engineering structures by component-wise models," *Journal of Sound and Vibration*, Vol. 333, No. 19, 2014, pp. 4597–4620. doi:10.1016/j.jsv.2014.04.063.

[37] Carrera, E., Filippi, M., Mahato, P. K. R., and Pagani, A., "Advanced models for free vibration analysis of laminated beams with compact and thin-walled open/closed sections," *Journal of Composite Materials*, Vol. 49, No. 17, 2014, pp. 2085–2101. doi:10.1177/0021998314541570.

[38] Carrera, E., and Petrolo, M., "Guidelines and Recommendations to Construct Theories for Metallic and composite plates," *AIAA Journal*, Vol. 48, No. 12, 2010, pp. 2852–2866. doi:10.2514/1.J050316.

[39] Bathe, K. J., *Finite element procedure*, Prentice Hall, Upper Saddle River, New Jersey, USA, 1996.

[40] Carrera, E., and Petrolo, M., "Refined Beam Elements with only Displacement Variables and Plate/Shell Capabilities," *Meccanica*, Vol. 47, No. 3, 2012, pp. 537–556. doi:10.1007/s11012-011-9466-5.

[41] Crisfield, M. A., "A fast incremental/iterative solution procedure that handles "snap-through"," *Computers & Structures*, Vol. 13, No. 1, 1981, pp. 55–62.

[42] Crisfield, M. A., "An arc-length method including line searches and accelerations," *International journal for numerical methods in engineering*, Vol. 19, No. 9, 1983, pp. 1269–1289.

[43] Carrera, E., "A study on arc-length-type methods and their operation failures illustrated by a simple model," *Computers & Structures*, Vol. 50, No. 2, 1994, pp. 217–229.

[44] Zienkiewicz, O. C., and Taylor, R. L., *The Finite Element Method for Solid and Structural Mechanics*, 6th ed., Butterworth-Heinemann, Washington, 2005.

[45] Flügge, W., *Stresses in shells*, 2nd ed., Springer, Berlin, 1960.

[46] Carrera, E., Cinefra, M., Petrolo, M., and Zappino, E., "Comparisons between 1D (Beam) and 2D (Plate/Shell) Finite Elements to Analyze Thin-Walled Structures," *Aerotecnica Missili e Spazio*, Vol. 93, No. 1-2, 2014, pp. 3–16.